

# Hydrodynamics of thermally-driven chiral propulsion and separation

E. Kirkinis,<sup>1,2,\*</sup> A. V. Andreev,<sup>3</sup> and M. Olvera de la Cruz<sup>1,2</sup>

<sup>1</sup>*Department of Materials Science & Engineering,  
Robert R. McCormick School of Engineering and Applied Science,  
Northwestern University, Evanston IL 60208 USA*

<sup>2</sup>*Center for Computation and Theory of Soft Materials,  
Northwestern University, Evanston IL 60208 USA*

<sup>3</sup>*Department of Physics, University of Washington, Seattle WA 98195 USA*  
(Dated: June 30, 2023)

Considerable effort has been directed towards the characterization of chiral mesoscale structures, as shown in chiral protein assemblies and carbon nanotubes. Here, we establish a thermally-driven hydrodynamic description for the actuation and separation of mesoscale chiral structures in a fluid medium. Cross flow of a Newtonian liquid with a thermal gradient gives rise to chiral structure propulsion and separation according to their handedness. In turn, the chiral suspension alters the liquid flow which thus acquires a transverse (chiral) velocity component. Since observation of the predicted effects requires a low degree of sophistication, our work provides an efficient and inexpensive approach to test and calibrate chiral particle propulsion and separation strategies.

Chirality, denoting the lack of superposition ability of structures on mirror images, is a characteristic of various assemblies including carbon nanotubes, viruses and actin filaments, and is essential for their function. Since left- and right-handed amino acids lead to different protein structures, their homochirality is required for biological function such as gene encoding [1]. Chiral proteins can sometimes lead to chiral mesoscale structures; some organisms with chiral body structures have chiral cells [2]. Therefore, the chirality of proteins may be responsible for the chiral mesoscale structures found in cell media. Chiral mesoscale assemblies are formed in peptide amphiphiles with chiral aminoacids [3] and in many carbon based systems, which have required great efforts to understand and characterize [4]. However, the mechanism by which chirality manifests at the mesoscale is not well understood. Here, we propose ways of actuating and separating mesoscale chiral structures such as helices [5], helicoidal scrolls [6] and twisted ribbons [7].

In chemical and biological systems various mesoscale structures move and function in an aqueous environment in the presence of thermal gradients induced by chemical reactions [8]. Temperature gradients may alter the liquid material parameters and in particular, viscosity, as this was demonstrated in laser-induced thermophoresis experiments [9] and the associated theory of a single hot particle in a viscous liquid [10]. This motivates us to study the *hydrodynamic* motion of chiral suspensions in Stokes flow in the presence of temperature gradients. The corresponding chiral current  $\mathbf{j}^{\text{ch}}$  is perpendicular to the plane formed by the base flow direction and the temperature gradient (cf. Fig. 1). The motion of the chiral suspension also perturbs the base flow and endows it with a transverse (chiral) velocity component. It is noteworthy that the chiral suspension also exerts a screw torque

on the confining walls, in the direction of the base flow. The hydrodynamic description developed in this article implies averaging over the tumbling motion of the chiral particles and applies at time scales longer than the tumbling time [11]. It can be understood as a “continuum” formulation for the motion of a chiral suspension and thus *differs* from the majority of propulsion descriptions which are based on a resistance matrix at the level of a single suspended particle [12]. The equivalence of the two approaches was discussed in the recent review article by Witten and Diamant [13].

Motion of chiral particles suspended in a classical liquid is associated with a chiral current and in particular  $\mathbf{j}^{\pm} = n^{\pm} \mathbf{v}_p^{\pm}$  where  $n^{\pm}$  is the number density of right and left-handed particles, respectively and  $\mathbf{v}_p^{\pm}$  is their respective velocity. For simplicity we consider an incompressible liquid where the right and left-handed particles are mirror-images of each other. We can thus define a chiral current  $\mathbf{j}^{\text{ch}}$  (cf. Fig. 1) of the form

$$\mathbf{j}^{\text{ch}} = \mathbf{j}^{+} - \mathbf{j}^{-}. \quad (1)$$

In the presence of temperature gradients a phenomenological expression for the chiral current  $\mathbf{j}^{\text{ch}}$  based on symmetry considerations and which has a low power of derivatives of vorticity is

$$\mathbf{j}^{\text{ch}} = \frac{n}{T} [\beta_1 (\nabla T \cdot \nabla) \text{curl} \mathbf{v} + \beta_2 \nabla T \times \nabla^2 \mathbf{v}], \quad (2)$$

where  $n = n^{+} + n^{-}$  and  $T, \mathbf{v}$  are the liquid’s, undisturbed by chirality, temperature and velocity respectively.  $\beta_{1,2}$  are described below. As mentioned above, the magnitude of the chiral current is determined by the complicated tumbling motion of the particles caused by thermal fluctuations and the inhomogeneous flow. The phenomenological expression (2) is written to lowest order in the driving flow. At strong drives thermal fluctuations are subdominant, and the magnitude of the chiral current is determined by averaging over corresponding Jeffery

\* kirkinis@northwestern.edu

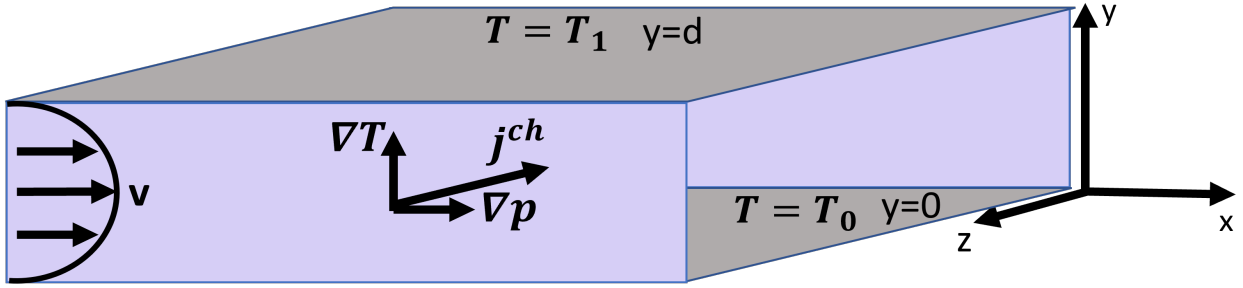


FIG. 1. A chiral current  $j^{\text{ch}}\hat{\mathbf{z}}$  of  $n$  chiral particles suspended in a classical liquid is induced by a vertical temperature gradient  $\nabla T = \partial_y T \hat{\mathbf{y}}$  and shear flow  $\mathbf{v} = u(y)\hat{\mathbf{x}}$ . In a nonracemic suspension of chiral particles the liquid is also perturbed by chirality and acquires a transverse chiral velocity component  $\delta v(y)\hat{\mathbf{z}}$  perpendicular to the direction of the base flow  $u(y)\hat{\mathbf{x}}$ .

orbits in the nonuniform flow. This problem, but in a different context, was discussed in [14].

In Ref. [11] the chiral current in an isothermal system was shown to be described by the expression

$$\mathbf{j}^{\text{ch}} = n\beta\nabla^2\text{curl}\mathbf{v}. \quad (3)$$

Insight into the physical origin of Eq.(2) may be obtained by applying Eq.(3) to a shear flow in the presence of temperature gradients. In particular, allowing temperature dependence of the liquid viscosity  $\eta$  and implementing the resulting vorticity equation, Eq.(3) leads to

$$\mathbf{j}^{\text{ch}} \sim n\beta\frac{\eta'}{\eta} [\nabla T \times \nabla^2\mathbf{v} + (\nabla T \cdot \nabla)\text{curl}\mathbf{v}], \quad (4)$$

where a prime denotes differentiation with respect to temperature  $T$  and we retained only leading order terms in temperature gradients. Thus, the coefficients  $\beta_1$  and  $\beta_2$  in (2) can be expressed in terms of the logarithmic derivative of viscosity with respect to temperature. We note that in the absence of temperature gradients chiral separation is possible only in nonstationary or nonlinear flows [11] as can be seen by the vorticity equation and (3). In the presence of temperature gradients chiral separation is possible even in the creeping flow regime. This is important for biological systems, which operate at low Reynolds numbers.

Recent literature examines the way microorganisms and active particles move in liquids with spatially-varying viscosity [9, 10, 15]. In what follows we are primarily concerned with suspensions where the viscosity  $\eta$  of the base liquid varies with temperature. A temperature gradient will then give rise to a chiral current of the forms (3) and (4).

The chiral density  $n^{\text{ch}} = n^+ - n^-$  satisfies the conservation law [11]

$$\partial_t n^{\text{ch}} + \text{div}(\mathbf{v}n^{\text{ch}}) + \text{div}[\mathbf{j}(n^{\text{ch}}) + \mathbf{j}^{\text{ch}}(n)] = 0, \quad (5)$$

where  $\mathbf{j}(n^{\text{ch}}) = -D\nabla n^{\text{ch}} - n^{\text{ch}}\lambda_T\nabla T - n^{\text{ch}}\lambda_p\nabla p$ , is the diffusive current relative to the liquid [11, 16] and  $\mathbf{j}^{\text{ch}}(n)$  is Eq. (3). The density  $n$  of chiral particles satisfies a similar conservation law, which is affected by chirality in a non-racemic mixture

$$\partial_t n + \text{div}(\mathbf{v}n) + \text{div}[\mathbf{j}(n) + \mathbf{j}^{\text{ch}}(n^{\text{ch}})] = 0, \quad (6)$$

so that Eq. (5) and (6) satisfy the Onsager principle of the symmetry of the kinetic coefficients [16].

A chiral suspension imparts stresses on the suspending liquid. To leading order in velocity gradients these stresses, allowed by symmetry, read

$$\begin{aligned} \sigma_{ij}^{\text{ch}} = & \eta(T)n^{\text{ch}} \{ \alpha [\partial_i(\text{curl}\mathbf{v})_j + \partial_j(\text{curl}\mathbf{v})_i] \\ & + \frac{\alpha_1}{T} [\epsilon_{kli}V_{kj} + \epsilon_{klj}V_{ki}] \partial_l T \}, \end{aligned} \quad (7)$$

where  $V_{ij}$  is the rate-of-strain tensor. The first term of Eq. (7) introduced in [11] was discussed in the recent review [13]. The second term exists only when temperature gradients are present in the liquid.

The coefficients  $\beta$ ,  $\alpha$  and  $\alpha_1$  in (3) and (7) are determined in the low Reynolds number regime by studying the particle motion in the surrounding liquid [12]. They may be estimated as

$$\alpha \sim \alpha_1 \sim \chi R^4 \quad \text{and} \quad \beta \sim \chi R^3, \quad (8)$$

where  $R$  is the chiral particle radius and  $\chi$  is the degree of chirality in the shape of the particles. Eq. (8) provides the order of magnitude estimates of these coefficients. Their precise determination for a specific particle shape however requires solving hydrodynamic equations for a tumbling particle in the presence of temperature and velocity gradients, and is beyond the scope of our work.

In the *absence* of chirality the liquid satisfies the Navier-Stokes equations and is considered incompressible

$$\rho Du_i/Dt = \partial_k \sigma_{ik} \quad \text{and} \quad \partial_i u_i = 0, \quad (9)$$

where the Cauchy stress tensor  $\sigma_{ik}$  is given by  $\sigma_{ik} = -p\delta_{ik} + \eta \left( \frac{\partial u_i}{\partial x_k} + \frac{\partial u_k}{\partial x_i} \right)$ ,  $i, k = 1, 2, 3$ ,  $\rho$  the density of the liquid and  $p$  is the pressure. Conservation of energy in an incompressible liquid is expressed in the form [16]

$$\rho c_p (\partial_t T + \mathbf{v} \cdot \text{grad}T) = k_{th} \nabla^2 T \quad (10)$$

where  $c_p$  is the specific heat at constant pressure and  $k_{th}$  the thermal conductivity of the liquid.

Consider pressure-driven flow, in the absence of chiral particles, in a channel with unevenly heated walls (cf. Fig. 1). With  $\mathbf{v} = u(y)\hat{\mathbf{x}}$ ,  $\nabla T = \partial_y T \hat{\mathbf{y}}$ , the Navier-Stokes

equations (9) and energy balance (10) in the creeping flow approximation reduce to

$$\frac{d}{dy} \left[ \eta(T) \frac{du}{dy} \right] = \frac{dp}{dx}, \quad \frac{d^2 T}{dy^2} = 0, \quad (11)$$

respectively, with boundary conditions

$$u(0) = u(d) = 0, \quad T(0) = T_0, \quad T(d) = T_0 + \Delta T. \quad (12)$$

The temperature profile thus obtained is  $T(y) = T_0 + \frac{y}{d} \Delta T$ . The solution of the first of Eq. (11) with boundary conditions (12) becomes

$$u(y) = \frac{T_e^2 d^2 \partial_x p}{2\eta(T)(\Delta T)^2} \frac{\sum_{\{i,j,k\}} e^{X_i} \left\{ \text{Ei}_1(X_i) \left[ \frac{e^{X_j}}{X_k^2} - \frac{e^{X_k}}{X_j^2} \right] + \frac{1}{X_j X_k} \left( \frac{1}{X_k} - \frac{1}{X_j} \right) \right\}}{[\text{Ei}_1(X_0) - \text{Ei}_1(X_1)] e^{X_0 + X_1} + \frac{e^{X_0}}{X_1} - \frac{e^{X_1}}{X_0}}, \quad (13)$$

where the symbol  $\{i, j, k\}$  denotes cyclic permutation of  $i, j$  and  $k$ , and  $\text{Ei}_1(X) = \int_1^\infty \frac{e^{-kX}}{k} dk$  is the exponential integral. Here we employed the well-documented Arrhenius-type law [17]

$$\eta(T) = \eta_0 e^{\frac{E}{R_g(T+T_A)}}, \quad (14)$$

valid in the 243 to 373 K temperature range, since it encompasses linear and other exponential laws [18], as special cases.  $E$  is the activation energy,  $R_g$  is the gas constant and  $T_A$  is a temperature correction, unique

to each viscous liquid, cf. [17] and Table I. In Eq. (13)  $X_i = \frac{T_e}{T_A + T_i}$ ,  $i = 0, 1, 2$ ,  $T_e = \frac{E}{R_g}$ , where  $T_0$  and  $T_1 = T_0 + \Delta T$  are the lower and upper channel wall fixed temperatures, respectively (cf. Fig. 1) and  $T_2 \equiv T = T_0 + \frac{y}{d} \Delta T$ .

Now consider the presence of chiral particles and define the chiral separation velocity

$$\mathbf{v}^{\text{ch}} \equiv \mathbf{j}^{\text{ch}}/n \quad (15)$$

relative to the liquid by employing (3). With respect to the geometry displayed in Fig. 1 it has the form  $\mathbf{v}^{\text{ch}} = v^{\text{ch}}(y) \hat{\mathbf{z}}$  and its magnitude is

$$v^{\text{ch}}(y) = \chi \frac{R^3 X_2^4 \Delta T \partial_x p}{d 2\eta(T) T_e} \frac{[\text{Ei}_1(X_1) - \text{Ei}_1(X_0)] e^{X_0 + X_1} + \sum_{i \neq j=0,1} \frac{(-1)^i e^{X_j}}{X_i^2} \left[ \frac{1}{2} + \frac{1}{X_i} \left( \frac{1}{X_2} - \frac{1}{2} \right) \right]}{[\text{Ei}_1(X_0) - \text{Ei}_1(X_1)] e^{X_0 + X_1} + \frac{e^{X_0}}{X_1} - \frac{e^{X_1}}{X_0}}. \quad (16)$$

In Fig. 2 we plot the closed form expression (16) for the chiral separation velocity  $v^{\text{ch}}$  in cm/sec vs. channel elevation  $y$  in cm for two temperature variations  $\Delta T$  between the lower (at  $y = 0$ ) and upper (at  $y = 0.1$  cm) channel walls. The chiral separation velocity is non-zero close to the solid walls located at  $y = 0, d$ , even though no-slip boundary conditions are satisfied by the base liquid. This is the case because, according to Eq. (3), chiral particle velocities become prominent in the vicinity of large vorticity gradients, and these are present close to the walls.

To obtain a better understanding of the effect, we average (16) over the channel width  $d$  and expand with respect to  $\Delta T$  to obtain  $\langle v^{\text{ch}} \rangle \sim 2\chi R^3 \gamma \frac{\Delta T}{d} \frac{\partial_x p}{\eta}$ , to leading order in  $\Delta T$ . It is more illuminating however to replace the pressure gradient with a characteristic velocity  $U_0$  of Poiseuille flow by averaging the (undisturbed by chirality) base Poiseuille profile  $u \sim \frac{\partial_x p}{2\eta(T_0)}(y^2 - yd)$  over the channel width  $d$ . This gives  $U_0 = -\frac{\partial_x p}{12\eta(T_0)} d^2$ , and substi-

tuting into the expression for  $\langle v^{\text{ch}} \rangle$  we obtain the chiral separation velocity

$$\langle v^{\text{ch}} \rangle = 24\chi \left( \frac{R}{d} \right)^3 U_0 \gamma \Delta T, \quad (17)$$

where we defined the average of a function  $f(y)$  with respect to the channel width to be  $\langle f \rangle = \frac{1}{d} \int_0^d f(y) dy$ ,  $R$  is chiral particle size and  $d$  channel width.  $\gamma = E/[R_g(T_0 + T_A)^2]$  is the logarithmic derivative of the viscosity which arises from the linearization of (14)  $\eta(T) \sim \eta(T_0) [1 - \gamma(T - T_0)]$ .

Considering BM-4 oil [17],  $\Delta T = 10$  K and the values displayed in Table I, Eq. (17) leads to the estimate

$$v^{\text{ch}} \sim 2\chi \mu\text{m}/\text{sec}. \quad (18)$$

The Reynolds number is  $\text{Re} \sim 3.4 \times 10^{-3}$ . Analogous results can be derived for silicon oils employed in the experiments of Ehrhard [19] and other liquids reported in the literature [17]. Water can also be used, although

TABLE I. Definitions and material parameters [17]

Quantity	Value	Definition
$\eta$ (g cm <sup>-1</sup> sec <sup>-1</sup> )	2.03	viscosity of BM-4 oil at 25 °C [17]
$R$ (cm)	$5 \times 10^{-3}$	chiral particle radius
$d$ (cm)	0.1	channel width
$U_0$ (cm/sec)	0.1	Poiseuille velocity
$T_0$ (K)	298.15	lower channel wall temperature
$\gamma$ (K <sup>-1</sup> )	0.07	BM-4 oil [17]
$E$ (kJ/mol)	7.5	activation energy of BM-4 oil [17]
$R_g$ (J/(mol K))	8.31441	gas constant
$T_A$ (K)	-186	BM-4 oil temp. correction [17]
$n^{\text{ch}}$ (cm <sup>-3</sup> )	$R^{-3}$	chiral density $n^+ - n^-$
$n$ (cm <sup>-3</sup> )	$R^{-3}$	particle number density $n^+ + n^-$
$u$ (cm/sec)		basic shear flow velocity
$v^{\text{ch}}$ (cm/sec)		chiral separation velocity
$\delta v$ (cm/sec)		chiral correction to flow velocity

it leads to Reynolds numbers higher than those reported here.

*Perturbation of liquid velocity by the chiral suspension.*- A chiral suspension imparts stresses on the suspending liquid. To leading order in gradients of vorticity these stresses, allowed by symmetry are given by (7). The liquid velocity  $\mathbf{v}$  acquires a chirality-induced component  $\delta v$  perpendicular to the plane of the base flow

$$\mathbf{v} = u(y)\hat{\mathbf{x}} + \delta v(y)\hat{\mathbf{z}}. \quad (19)$$

With the correction (7) the Cauchy stress tensor reads

$$\sigma_{ij} = -p\delta_{ij} + \eta(\partial_i u_j + \partial_j u_i) + \sigma_{ij}^{\text{ch}}. \quad (20)$$

Conservation of linear momentum  $\partial_j \sigma_{ij} = 0$  along the flow direction  $\hat{\mathbf{x}}$ :  $-\partial_x p + \partial_y(\eta\partial_y u) = 0$ , is now accompanied by its chirality-induced counterpart that is perpendicular to the base flow direction

$$\hat{\mathbf{z}} : \partial_y(\eta\partial_y \delta v) - n^{\text{ch}}\chi R^4 \partial_y(\eta\partial_y^2 u) = 0, \quad (21)$$

and satisfies no-slip boundary conditions  $\delta v(0) = \delta v(d) = 0$ . The solution  $\delta v$  of Eq. (21) is displayed in Fig. 3 in cm/sec vs. channel elevation  $y$  in cm for two temperature variations  $\Delta T$  between the lower (at  $y = 0$ ) and upper (at  $y = 0.1$  cm) channel walls, employing the Arrhenius-type temperature dependent viscosity law (14). Its profile is skewed due to the reduction of viscosity close to the upper heated channel wall which is also the location of high chiral separation velocity  $v^{\text{ch}}$ . To leading order in  $\Delta T$ , and averaging over the channel width  $d$ , we obtain  $\langle \delta v \rangle \sim \chi R \frac{d\partial_x p}{12\eta} \gamma \Delta T$ . Replacing the pressure gradient with its Poiseuille flow counterpart, leads to

$$\langle \delta v \rangle \sim \chi \frac{R}{d} U_0 \gamma \Delta T. \quad (22)$$

Employing the material parameters for BM-4 oil displayed in Table I and setting  $\Delta T = 10$  K we obtain  $\delta v \sim 35\chi \mu\text{m}/\text{sec}$ , which agrees well, in order of magnitude, with the exact solution displayed in Fig. 3. The

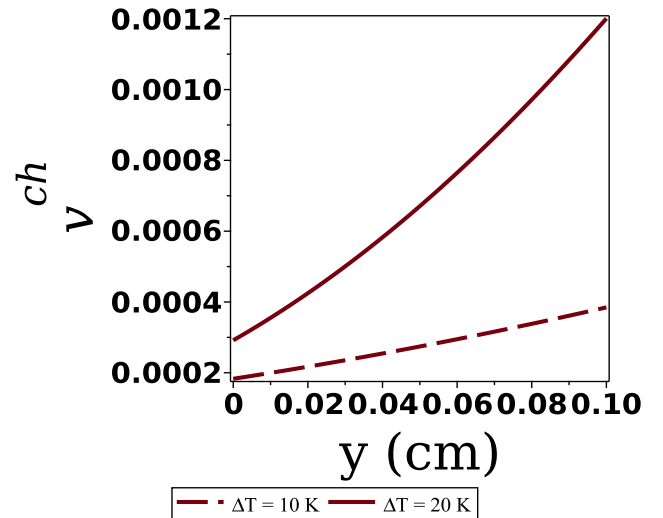


FIG. 2. Chiral separation velocity  $v^{\text{ch}}$  in cm/sec from Eq. (16), perpendicular to the  $x$ - $y$  plane formed by a base Poiseuille flow and the vertical temperature gradient directions (cf. Fig.1).  $y$  is vertical channel coordinate in cm and we employed the Arrhenius-type temperature dependent viscosity law (14) for a BM-4 oil [17].  $\chi$  has been set equal to 1.

momentum equation displayed in (21) was formulated by considering only the first term of the constitutive law (7) since the second term, and for the material parameters employed in this article, gives velocities that are one order of magnitude smaller than the ones derived here.

*Screw torque in a non-racemic suspension.*- A non-racemic mixture will apply shear stresses on the channel walls that are perpendicular to the plane of the paper. These forces arise from the chiral momentum flux density (7), cf. [11]. Employing the geometry of the channel Poiseuille flow displayed in Fig. 1 this stress is

$$\hat{\mathbf{z}} : \sigma_{zy}^{\text{ch}} = \chi R \eta \partial_y^2 u. \quad (23)$$

In Fig. 4 we display the chiral stress  $\sigma_{zy}^{\text{ch}}$  as a function of channel width employing the exact form for the liquid velocity profile (13). Since the normal vectors to the two channel walls have opposite sign, the chiral suspension exerts on the walls two forces of opposite sign directed into and out of the page. Hence, there is a screw torque exerted by the chiral flow on the confining walls and is directed along the  $\hat{\mathbf{x}}$  direction of the flow. The average of the chiral stress  $\langle \sigma_{zy}^{\text{ch}} \rangle$  over the channel width to leading order in  $\Delta T$  becomes

$$\langle \sigma_{zy}^{\text{ch}} \rangle = \chi R \partial_x p \left( 1 + \frac{1}{2} \gamma \Delta T + O((\Delta T)^2) \right). \quad (24)$$

Expression (24) implies that a chiral stress exists even in the absence of temperature gradients. This was also noted in [11]. Replacing the pressure gradient by the base Poiseuille profile, as carried out in the foregoing sections and employing the material values appearing in Table I

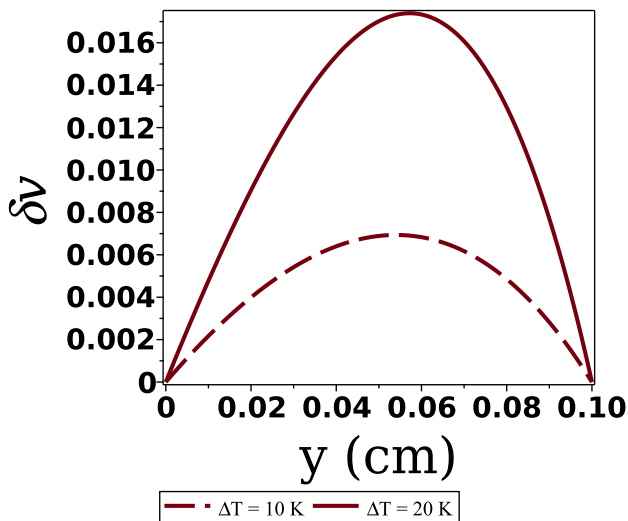


FIG. 3. Transverse chiral component of liquid velocity  $\delta v$  in cm/sec, perpendicular to the  $x$ - $y$  plane formed by a Poiseuille flow and the temperature gradient directions (cf. Fig.1) and obtained by solution of Eq. (21) with boundary conditions  $\delta v(0) = \delta v(d = 0.1) = 0$ .  $y$  is vertical channel coordinate in cm and we employed the Arrhenius-type temperature dependent viscosity law (14) for a BM-4 oil [17] giving rise to the skewness of chiral velocity profiles.  $\chi$  has been set equal to 1.

for  $\Delta T = 10K$ , Eq.(24) gives  $\langle \sigma_{zy}^{\text{ch}} \rangle = 1.73\chi$  dynes/cm<sup>-2</sup>. This estimate agrees, in order of magnitude, with those of same-size systems known in the literature [20].

We note the existence of a related thermal effect for the propulsion of chiral particles when the viscosity is temperature-dependent and thermal gradients are generated at the interior by viscous heating [21]. The energy equation is now replaced by  $\kappa \partial_y^2 T + \eta(T) (\partial_y u)^2 = 0$ , where  $\kappa$  is the thermal conductivity of the liquid. The external stimuli may be supplied, for instance, by sliding one channel wall at constant speed  $V$ . In this case the vorticity equation and the chiral current depend on the Brinkman number  $Br$ , that is, the ratio of viscous heating to conduction  $Br = \frac{\eta V^2}{\kappa}$ . The chiral separation velocity becomes  $v^{\text{ch}} \sim \frac{\chi}{8} \left(\frac{R}{d}\right)^3 Br$ .

Another related thermally-induced chiral particle propulsion effect can take place in a Rayleigh-Bénard cell [22], driven by variations of the liquid density with tem-

perature. Here, the coefficient of thermal expansion  $\alpha_T$  is the logarithmic derivative of density with respect to temperature, in the same sense that  $\gamma$  in Eq. (17) is the logarithmic derivative of viscosity. Diffusion of vorticity, perpendicular to the plane of the cell, is now induced by  $\rho \alpha_T \nabla T \times \mathbf{g}$ , where  $\rho$  is the unperturbed mass density of the liquid and both the temperature gradient and gravitational acceleration  $\mathbf{g}$  lie on the plane of the cell. The chiral separation velocity is  $v^{\text{ch}} \sim \chi \frac{R^3 \rho g \alpha_T \Delta T}{\eta d}$ . This effect is present when the Rayleigh number exceeds its

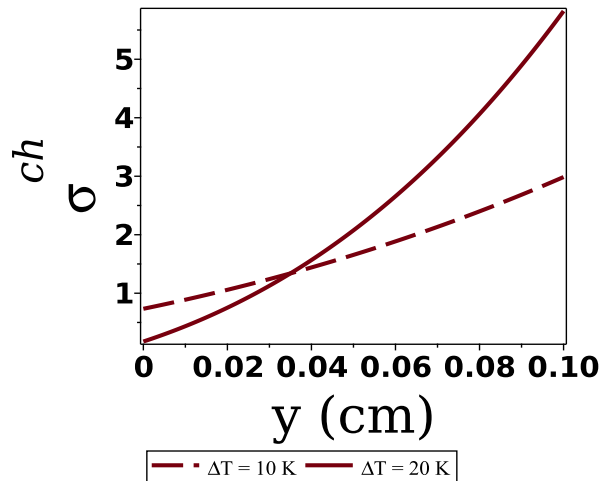


FIG. 4. Distribution of the chiral stress  $\sigma_{zy}^{\text{ch}}$  in (23) in dynes/cm<sup>2</sup> imparted by the chiral suspension on the liquid in a direction perpendicular to the  $x$ - $y$  plane formed by the Poiseuille flow and the vertical temperature gradient (cf. Fig.1), vs. the vertical coordinate  $y$  of the channel in cm and we employed the Arrhenius-type temperature dependent viscosity law (14) for a BM-4 oil [17]. Since the normal vectors to the two channel walls have opposite signs, the chiral suspension exerts on the walls two forces of opposite sign directed into and out of the page. Hence, there is a screw torque exerted by the chiral flow on the confining walls and is directed along the base flow direction.  $\chi$  has been set equal to 1.

critical value.

We thank the Department of Energy, Office of Basic Energy Sciences for support under contract DE-FG02-08ER46539 (M.O.C and E.K.). The work of A.V.A. was supported, in part, by the US National Science Foundation through the MRSEC Grant No. DMR-1719797.

[1] M. Inaki, J. Liu, and K. Matsuno, Philosophical Transactions of the Royal Society B: Biological Sciences **371**, 20150403 (2016).  
 [2] J. Fan, H. Zhang, T. Rahman, D. Stanton, and L. Wan, Communicative & Integrative Biology **12**, 78 (2019).  
 [3] C. Gao, S. Kewalramani, D. Valencia, H. Li, J. McCourt, M. Olvera de la Cruz, and M. Bedzyk, Proceedings of the

National Academy of Sciences **116**, 22030 (2019).  
 [4] M. Arnold, A. Green, J. Hulvat, S. Stupp, and M. Hersam, Nature nanotechnology **1**, 60 (2006).  
 [5] T. Shimizu, M. Masuda, and H. Minamikawa, Chemical Reviews **105**, 1401 (2005); J. McCourt, S. Kewalramani, C. Gao, E. Roth, S. Weigand, M. Olvera de la Cruz, and M. Bedzyk, ACS Central Science **8**, 1169 (2022).

- [6] K. Nagarsekar, M. Ashtikar, F. Steiniger, J. Thamm, F. Schacher, and A. Fahr, *Soft Matter* **12**, 3797 (2016).
- [7] R. Oda, I. Huc, M. Schmutz, S. Candau, and F. MacKintosh, *Nature* **399**, 566 (1999).
- [8] H. Zhang, W. Duan, M. Lu, X. Zhao, S. Shklyaev, L. Liu, T. Huang, and A. Sen, *ACS Nano* **8**, 8537 (2014).
- [9] R. Schermer, C. Olson, J. Coleman, and F. Bucholtz, *Optics Express* **19**, 10571 (2011).
- [10] N. Oppenheimer, S. Navardi, and H. Stone, *Physical Review Fluids* **1**, 014001 (2016).
- [11] A. Andreev, D. Son, and B. Spivak, *Physical Review Letters* **104**, 198301 (2010).
- [12] J. Happel and H. Brenner, *Low Reynolds number hydrodynamics with special applications to particulate media* (Prentice-Hall Inc., Englewood Cliffs, N.J., 1965) pp. xiii+553.
- [13] T. Witten and H. Diamant, *Reports on Progress in Physics* **83**, 116601 (2020).
- [14] E. Kirkinis, A. Andreev, and B. Spivak, *Physical Review E* **85**, 016321 (2012).
- [15] C. Datt and G. Elfring, *Physical Review Letters* **123**, 158006 (2019); K. Shoele and P. Eastham, *Physical Review Fluids* **3**, 043101 (2018).
- [16] L. D. Landau and E. M. Lifshitz, *Fluid Mechanics. Course of Theoretical Physics, Vol. 6* (Pergamon Press Ltd., London-Paris, 1987) pp. xii+515.
- [17] R. Fogel'son and E. Likhachev, *Technical Physics* **46**, 1056 (2001).
- [18] M. Potter and E. Graber, *The Physics of Fluids* **15**, 387 (1972); S. Davis, G. Kriegsmann, R. Laurence, and S. Rosenblat, *ibid.* **26**, 1177 (1983); D. Wall and S. Wilson, *Journal of Fluid Mechanics* **323**, 107 (1996).
- [19] P. Ehrhard, *Journal of Fluid Mechanics* **257**, 463 (1993).
- [20] D. Kataoka and S. Troian, *Nature* **402**, 794 (1999); J. Ando and K. Yamamoto, *Circulation Journal* **73**, 1983 (2009).
- [21] E. Kirkinis and A. Andreev, *Journal of Fluid Mechanics* **872**, 308 (2019).
- [22] S. Chandrasekhar, *Hydrodynamic and hydromagnetic stability* (Oxford University Press, 1961).